Thermochimica Acta 499 (2010) 111–116

Contents lists available at ScienceDirect

Thermochimica Acta

journal homepage: www.elsevier.com/locate/tca

Combustion synthesis and effect of $LaMnO_3$ and LaOCl powder mixture on HMX thermal decomposition

Zhi-Xian Wei[a,*], Yan Wang[a], Xue-Jun Zhang[a], Chang-Wen Hu[b,*]

[a] Department of Chemistry, Science Institute, North University of China, Taiyuan, Shanxi 030051, PR China
[b] Department of Chemistry and The Institute for Chemical Physics, Beijing Institute of Technology, Beijing, 100081, PR China

ARTICLE INFO

Article history:
Received 20 August 2009
Received in revised form
15 November 2009
Accepted 24 November 2009
Available online 3 December 2009

Keywords:
Stearic acid gel
Combustion synthesis
Perovskite-type $LaMnO_3$
HMX

ABSTRACT

LaOCl powder mixture and perovskite-type $LaMnO_3$ were prepared by stearic acid gel combustion method. The obtained powders were characterized by X-ray powder diffraction (XRD), scanning electron microscopy (SEM), Fourier transform infrared (FT-IR) and X-ray photoelectron spectroscopy (XPS) techniques. LaOCl powder mixture was a mixture of LaOCl and significant amounts of amorphous materials. When heated at 973.15 K, the mixture was found to be converted into single-phase perovskite-type $LaMnO_3$. The catalytic activities of LaOCl powder mixture and $LaMnO_3$ were investigated for octahydro-1,3,5,7-tetranitro-1,3,5,7-tetrazocine (HMX) thermal decomposition by thermal gravity (TG) and thermogravimetry-evolved gas analysis (TG–EGA) techniques. The experimental results show that both the mixture and $LaMnO_3$ have catalytic activities for the thermal decomposition of HMX, and LaOCl powder mixture has much higher catalytic activity than $LaMnO_3$ on the early stages of HMX thermal decomposition. That could be attributed to the higher surface adsorption oxygen (O_{ad}) and hydroxyl as well as its high specific surface area. $LaMnO_3$ can obviously reduce activation energy of HMX thermal decomposition than LaOCl powder mixture. This may be due to its catalytic activity on the oxidation reaction of CO and the reaction between CO and NO during HMX thermal decomposition.

1. Introduction

ABO_3 perovskite-type oxides with A as La, B as transition metal are widely used in many fields. In particular, they can display prominent catalytic activities. For example, they have been used as catalysts for the auto-reforming of sulfur containing fuels [1], for catalyzing the reaction between CO and NO_x in the auto emission [2] and for the total oxidation of methane and volatile organic compounds [3]. However, one of the technical constraints to the use of perovskite-type catalysts is the inability to produce high specific surface area powders.

Structures and properties of ABO_3 oxides are strongly influenced by the synthesis methods. The $LaMnO_3$ and related compounds have been synthesized by many methods, including sol–gel method, flame hydrolysis from aqueous solution, complexation through EDTA as well as solid-state reaction [4] and solution combustion synthesis [5]. Of these methods, solution combustion synthesis is particularly suited to produce nanosized powders. However, conventional solution combustion route is aqueous solution synthesis, so the hydrolysis of the metal ions is unavoidable, which easily leads to the inhomogeneity of the phase. To avoid the disadvantages of aqueous solution combustion synthesis, we prepared perovskite-type $LaMnO_3$ and LaOCl powder mixture with high specific surface areas by stearic acid gel combustion method, where stearic acid was used as reaction solvent, dispersant, complexing agent.

Octahydro-1,3,5,7-tetranitro-1,3,5,7-tetrazocine (HMX) is one of the major ingredients in nitrate ester plasticized polyether (NEPE) propellant. The primary drawbacks of NEPE propellant are high pressure index (n) values [6] and the difficulty of modification of burning rate due to the high content of HMX [7]. Catalytic behavior for HMX thermal decomposition of additives or catalysts could control the burning rate and influence the combustion behavior of NEPE propellant. So, catalysis of HMX thermal decomposition is of interest.

Perovskite-type oxides $LaMnO_3$ and related compounds are capable of catalyzing the reaction between CO and NO_x in the auto emission [2]. Note that CO and NO_x are also two major products of HMX thermal decomposition. It has been put forward that, if the reaction can be catalyzed between CO and NO_x on the burning surface of NEPE propellant, the pressure index will be reduced [8]. So it is anticipated to use perovskite-type oxides as novel catalysts or modifiers for NEPE propellant.

The catalytic activities of some additives or catalysts such as perovskite-type $LaFeO_3$ and metal formiates on the thermal decomposition of HMX have been reported [9–11]. In order to search

* Corresponding authors. Tel.: +86 0351 3921414; fax: +86 0351 3921414.
E-mail address: zx_wei@126.com (Z.-X. Wei).

0040-6031/$ – see front matter © 2009 Elsevier B.V. All rights reserved.
doi:10.1016/j.tca.2009.11.010

more additives or catalysts for HMX thermal decomposition, LaOCl powder mixture and perovskite-type $LaMnO_3$ were investigated for HMX thermal decomposition in this study.

2. Experimental

2.1. Auto-combustion synthesis of LaOCl powder mixture and perovskite-type $LaMnO_3$

$MnCl_2{\cdot}4H_2O$, $La(NO_3)_3{\cdot}6H_2O$ and stearic acid were analytical grade chemicals and were used as raw materials to prepare LaOCl powder mixture and perovskite-type $LaMnO_3$. First, $MnCl_2{\cdot}4H_2O$ and $La(NO_3)_3{\cdot}6H_2O$ with Mn/La molar ratio of 1/1 were added into the little excess molten stearic acid in a porcelain crucible reactor. After that, the resulting mixture was continuously stirred and kept at 391.15 K for a sufficient period of time to allow the gel to be formed. Then, the porcelain crucible reactor was placed on a hot plate increased to 773.15 K. At this stage, the stearic acid gel volatilized and autoignited, with the evolution of a large volume of gases to produce loose powder, i.e., LaOCl powder mixture. After the mixture powder was calcined at 973.15 K for 1 h, perovskite-type $LaMnO_3$ was obtained.

2.2. Powders characterization

The composition and phase purity of obtained powders were examined by X-ray diffractometer (Cu Kα = 1.54 Å, 40 kV, 30 mA, 2θ from 10° to 80°). FT-IR spectra were registered by using a Nexus 870 FT-IR in KBr pellets. The BET specific surface areas of the obtained powders were evaluated from the linear parts of the BET plot of the N_2 isotherms, using a NOVA4200e analyzer. Scanning electron microscopy (SEM) (HITACHA, Model S-4800) was used to investigate the morphology of obtained powders. XPS analysis was performed by a PHI Quantera SXM apparatus, equipped with a standard Al Kα excitation source. The binding energy (BE) scale has been calibrated by measuring C 1s peak (BE = 284.8 eV) from the ubiquitous surface layer of adventitious carbon.

2.3. Catalytic activity test

The obtained powders and HMX (Xingan Chemical Industry Company) were mixed in 2:98 (wt.%), respectively by rubbing method to prepare the samples for a series of TG and TG–EGA experiments.

TG measurements were performed at temperature-programmed rate of 5 K min^{-1} in N_2 atmosphere with a flow rate of 50 mL min^{-1} over the range of room temperature to 623.15 K on a Perkin-Elmer pyris 1 TGA, and ~0.5 mg of sample was used in open Al-crucibles. The TGA instrument was calibrated for temperature response using the Curie points of nickel and iron.

In addition, the catalytic activity of LaOCl powder mixture was tested by TG–EGA technique. The experiments were carried out using a Perkin-Elmer Pyris Diamond TG equipped with a ThermoStar mass spectrometer for analysis of gases evolved during the samples heating. The temperature-programmed rate was 10 K min^{-1} in the temperature range room temperature to 473.15 K and then 5 K min^{-1} in the temperature range 473.15–623.15 K in nitrogen with a flow rate of 100 mL min^{-1}, and 10 mg sample was used. Gaseous products were continually monitored for chosen mass numbers m/z (27-HCN^+, 30-NO^+ and 30-$HCHO^+$), which are several products from the solid and liquid phase thermal decomposition of HMX and not present on the surface of the mixture powder.

All the experiments were repeated twice.

3. Results and discussion

3.1. Phase composition and microstructure of obtained powders

The X-ray diffraction patterns of LaOCl powder mixture and $LaMnO_3$ are shown in Fig. 1. The broad and poorly defined peaks in Fig. 1a correspond to LaOCl (PDF #64-7261). So, the mixture obtained by the combustion of the La–Mn–stearic acid gel is a mixture of LaOCl and significant amounts of amorphous materials. The LaOCl peaks are present after heating to 873.15 K and, additionally, intense peaks associated with the cubic perovskite structure emerge. By 973.15 K, the LaOCl has completely decomposed and the single-phase perovskite-type $LaMnO_3$ (PDF #75-0440, cubic, a = 3.880) is formed.

Fig. 2 shows the SEM images of LaOCl powder mixture and $LaMnO_3$. The mixture has morphology of thin flakes with a little amount of the spherical particles (Fig. 2a). $LaMnO_3$ has a well-developed spherical nanostructure with characteristic scale ~0.05–0.1 μm (Fig. 2b).

In this study, the specific surface areas of LaOCl powder mixture and $LaMnO_3$ calcined at 973.15 K for 1 h are 71.51 and 26.76 m^2/g, respectively. However, the corresponding values for $LaMnO_3$ prepared by oxalyl dihydrazide and urea aqueous solution combustion methods are 12.5 m^2/g [12] and 5.6 m^2/g [13], respectively. Obviously, the value in this study is higher. This indicates that stearic acid gel combustion is an effective way to prepare nano-meter/ultrafine powders.

3.2. FT-IR spectra

To detect the presence of surface species for the obtained powders, FT-IR spectra were recorded. As shown in Fig. 3a and b, the wide bands observed at about 3409 cm^{-1} are characteristic of the H–O bending mode of absorbed water or hydroxyl groups, and the bands observed at about 2359 cm^{-1} correspond to the physically surface-absorbed CO_2 (due to the deformation mode of gas-phase CO_2, unperfectly subtracted). The band at 1637 cm^{-1} corresponds to the surface-adsorbed oxygen species [14]. In Fig. 3a, the weak bands at around 1476 and 1391 cm^{-1} as well as smaller one at around 846 cm^{-1} are attributed to the principal vibrations of CO_3^{2-} groups, indicating La-carbonate species (i.e., $La_2O_2CO_3$) exist on the surface of LaOCl powder mixture. Here, the carbonation of La^{3+} would easily occur if the oxidation decomposition was performed in the CO_2-containing gas-phase (CO_2 comes from the oxidation decomposition of stearates) [15]. In addition, it can be seen that $LaMnO_3$

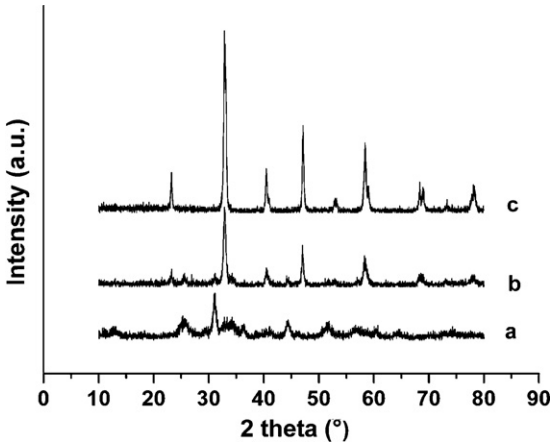

Fig. 1. XRD of obtained powders: LaOCl powder mixture (a), LaOCl powder mixture calcined at 873.15 K for 1 h (b) and LaOCl powder mixture calcined at 973.15 K for 1 h (c).

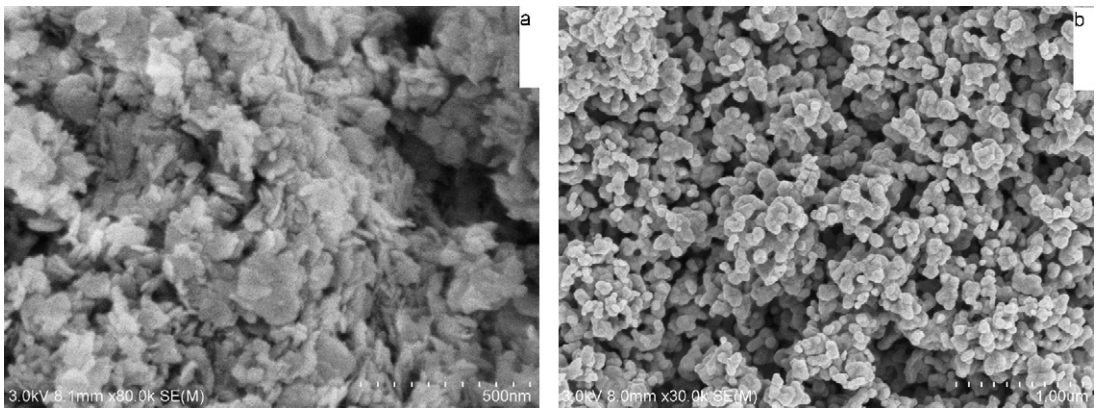

Fig. 2. SEM of obtained powders: LaOCl powder mixture ×80 K (a) and $LaMnO_3$ ×30 K (b).

has no obvious peaks of carbonate species. In Fig. 3a and b, the bands around 614 cm^{-1} correspond to the stretching mode of the Mn–O–Mn or Mn–O bond [12] and the band around 505 cm^{-1} is due to the principal vibration of La–O bond (Fig. 3a) in LaOCl [16]. These results show that the adsorbed water or hydroxyl groups, surface-adsorbed oxygen, and carbonate species exist on the surface of LaOCl powder mixture.

3.3. XPS studies

Fig. 4 shows the C 1s spectra of LaOCl powder mixture and $LaMnO_3$. C 1s signal in Fig. 4a and b located at 284.8 eV corresponds to the reference, and the higher one (around 289.7 eV) can be assigned to carbonated species [15], also indicating that lanthanum ion is highly reactive towards CO_2. A comparison of Fig. 4a and b suggests that LaOCl powder mixture has much higher carbonated species, in agreement with the results of FT-IR.

Fig. 5 shows the O 1s spectra of LaOCl powder mixture and $LaMnO_3$. In Fig. 5b, O 1s spectra of $LaMnO_3$ show two major components: One at 529.4 eV is attributable to the lattice oxygen O^{2-}, and the other broad peak at around 531.6 eV corresponds to surface-adsorbed oxygen species. Based on the results of FT-IR and C 1s spectra of $LaMnO_3$, the surface-adsorbed oxygen species consist of adsorbed oxygen (O_{ad}), hydroxyl groups or water, and traces of carbonated species. For LaOCl powder mixture, O 1s spectra (Fig. 5a) also show two major components: One at 529.4 eV is attributable to the lattice oxygen O^{2-}, and the other peak at around 531.6 eV corresponds to the surface-adsorbed species, which are comprised of adsorbed oxygen (O_{ad}), hydroxyl groups or water, and carbonate species (see Fig. 3a). A comparison of Fig. 5a and b replies that LaOCl powder mixture has much higher surface-adsorbed species.

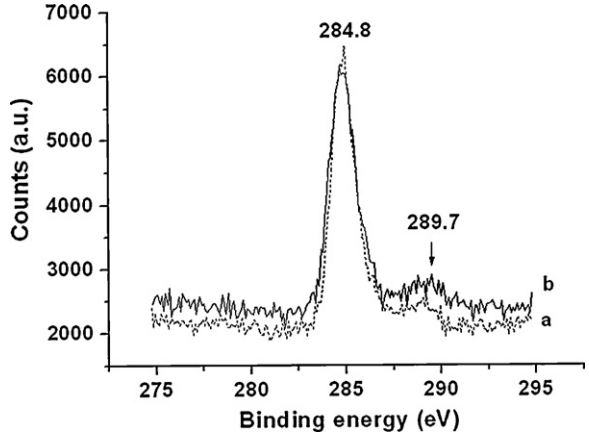

Fig. 4. C 1s XP spectra of LaOCl powder mixture (a) and $LaMnO_3$ (b).

3.4. Catalytic thermal decomposition of HMX

The catalytic activities of LaOCl powder mixture and $LaMnO_3$ for the thermal decomposition of HMX were studied by TG. As shown in Fig. 6, the onset temperature of HMX thermal decomposition is at 531.9 K, and the rate has a maximum at 562.2 K, which is obtained by DTG. The onset temperature in presence of LaOCl powder mix-

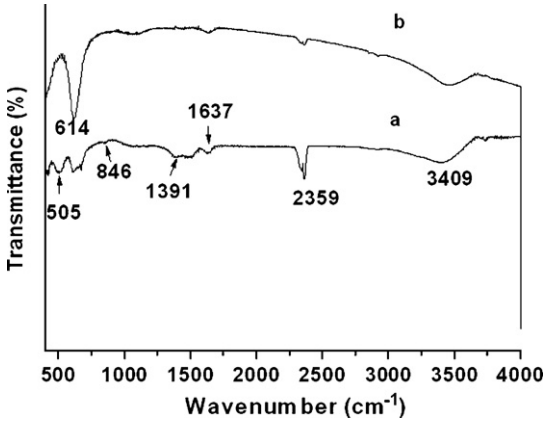

Fig. 3. FT-IR spectra of LaOCl powder mixture (a) and $LaMnO_3$ (b).

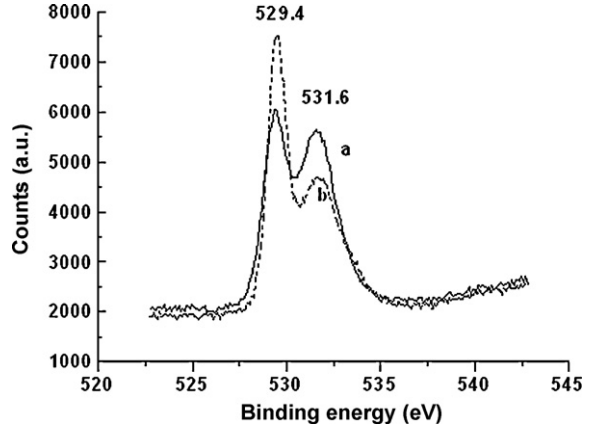

Fig. 5. O 1s XP spectra of LaOCl powder mixture (a) and $LaMnO_3$ (b).

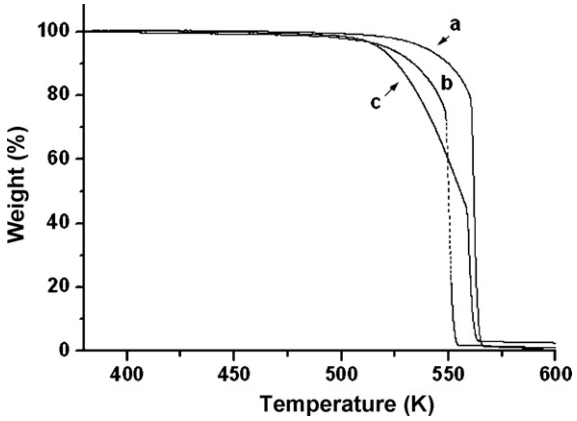

Fig. 6. TG curves of catalytic thermal decomposition of HMX in nitrogen: HMX (a), HMX + $LaMnO_3$ (b), HMX + LaOCl powder mixture (c).

ture is at 505.0 K, which is 26.9 K lower than that of HMX; the maximum is at 559.6 K, which is 2.6 K lower than that of HMX. The onset temperature with $LaMnO_3$ is at 509.1 K, which is 22.8 K lower than that of HMX; the maximum is at 550.4 K, which is 11.8 K lower than that of HMX. Obviously, the temperatures of the onset and the maximum mass-loss rate decrease by adding of LaOCl powder mixture and $LaMnO_3$. These experimental results show that LaOCl powder mixture and $LaMnO_3$ mainly catalyze the early stages (the solid phase) of HMX thermal decomposition (liquefaction temperatures 280–283 °C for HMX), and LaOCl powder mixture has much higher catalytic activity than $LaMnO_3$. After melting, autocatalytic reactions may occur in the course of the liquid phase decomposition of HMX.

In addition, the kinetic parameters (the activation energy E and the pre-exponential factor A) were calculated from TG traces using the Coats–Redfern equation.

Coats–Redfern relation is

$$\log\left[\frac{g(\alpha)}{T^2}\right] = \log\left[\frac{AR}{\beta E(1-2\bar{T}/E)}\right] - \frac{E}{2.303RT}$$

Here α denotes the fractional mass loss, R is the gas constant, T is the temperature in Kelvin at any instant, $\overline{T}$ is the mean experimental temperature, β is the heating rate, and $g(\alpha)$is the reaction model. Note that the sixteen forms of $g(\alpha)$, suggested by Satava [17] are used to enunciate the mechanism of thermal decomposition in each stage.

For the early stages of HMX thermal decomposition, a plot of L.H.S. of this equation against $1/T$ gives straight line whose slope and intercept are used for calculate the kinetic parameters by the least-square method. The correlation coefficient for all these forms were calculated and the forms of $g(\alpha)$ for which the correlation has a maximum value and the standard deviation has a minimum value are chosen as the mechanism of reaction. The various kinetic parameters calculated are given in Table 1.

Table 1 showed that LaOCl powder mixture and $LaMnO_3$ can reduce the activation energy of HMX thermal decomposition, and the decrease trend is more obvious for $LaMnO_3$ than for LaOCl powder mixture.

In the present investigation, the highest value of correlation coefficient and the lowest value of standard deviation are obtained for $g(\alpha) = \alpha$ for the early stages of HMX thermal decomposition. Hence, early stages of HMX thermal decomposition are controlled by the sublimation of HMX or adsorption and desorption of the gas products from HMX thermal decomposition. This is in agreement with the results in a previous paper [18].

The reaction model $g(\alpha)$ does not change for the thermal decomposition of HMX with LaOCl powder mixture when the α (fractional mass loss) in the range of 1–10%. However, when the α in the range of 10.0–45.4%, the highest value of correlation coefficient and the lowest value of standard deviation are obtained for

$$g(\alpha) = -\ln(1-\alpha)$$

in this stage. Hence, the mechanism is "random nucleation with one nucleus on each particle" representing 'Mampel model'.

For HMX in presence of $LaMnO_3$, the $g(\alpha)$ does not change, but the activation energy E is reduced obviously, indicating that $LaMnO_3$ has catalytic activity on the thermal decomposition of HMX.

We further tested catalytic activity of LaOCl powder mixture for HMX thermal decomposition by TG–EGA. The graphs of TG and EGA (the released degree of chosen gaseous products versus time) are displayed in Fig. 7. The difference of traces for TG shown in Fig. 7a from those in Fig. 6 is due to the different experimental instrument and the powder mass used in this study.

Fig. 7a shows that the beginning decomposition temperature of HMX decreases by adding of the LaOCl powder mixture. Fig. 7b and c indicates that HMX with LaOCl powder mixture decomposes first, and the ion current intensities of HCN and both NO and HCHO (they appeared in the same time scale, for they have the same mass numbers) are 3.12 and 2.94 times higher than those of HMX without LaOCl powder mixture, respectively. The increase in gas release indicates a more intense decomposition of HMX. Therefore, LaOCl powder mixture catalyzes HMX thermal decomposition.

Quantum chemical calculation [19] indicate that after a hydrogen atom is abstracted from the CH_2 group of HMX, the bond strength of the adjacent N–N bond drops to 8 kJ/mol, thus causing the NO_2 group to leave easily. Hydrogen atoms may be abstracted by radicals present in the gas-phase, such as OH and water. Water is one of the most abundant species during the early stages of HMX thermal decomposition. So Behrens concluded that OH and H_2O may initiate HMX thermal decomposition [19]. Also, it is reported that the N–N bond of HMX is easily ruptured at low pressure or constant-pressure [20]. Further, the presence of HCN (see Fig. 7) also implies dominant rupture of N–N bond in HMX.

Surface-adsorbed species such as adsorbed oxygen (O_{ad}), hydroxyl groups or water are weakly bounded on the powder surface and usually are considerate as the origin of the characteristic catalytic properties [21]. According to the Behrens viewpoint [19] and the mechanism of the early stages of HMX thermal decomposition (see Table 1), one can explain the possible reason of the catalytic effect of LaOCl powder mixture and $LaMnO_3$ on the early stages of HMX thermal decomposition. During the thermal decomposition of HMX in presence of $LaMnO_3$ or LaOCl powder mixture with increasing temperature, the desorbed gases such as

Table 1
Non-isothermal kinetic parameters of HMX mixtures at 5 K min^{-1} determined using the Coats–Redfern equation.

Samples	α (%)	T (K)	E_a (kJ mol^{-1})	$\log_A$ (min^{-1})	$g(\alpha)$
HMX	1.0–12.5	514.2–553.5	149.3	12.70	α
HMX + LaOCl	1.0–10.0	494.7–525.8	141.8	12.56	α
HMX + $LaMnO_3$	1.0–10.0	471.2–533.1	110.8	9.28	α
HMX + LaOCl	10.0–45.4	525.8–552.7	144.0	12.88	$-\ln(1-\alpha)$
HMX + $LaMnO_3$	10.0–23.8	533.2–548.6	120.1	10.20	α

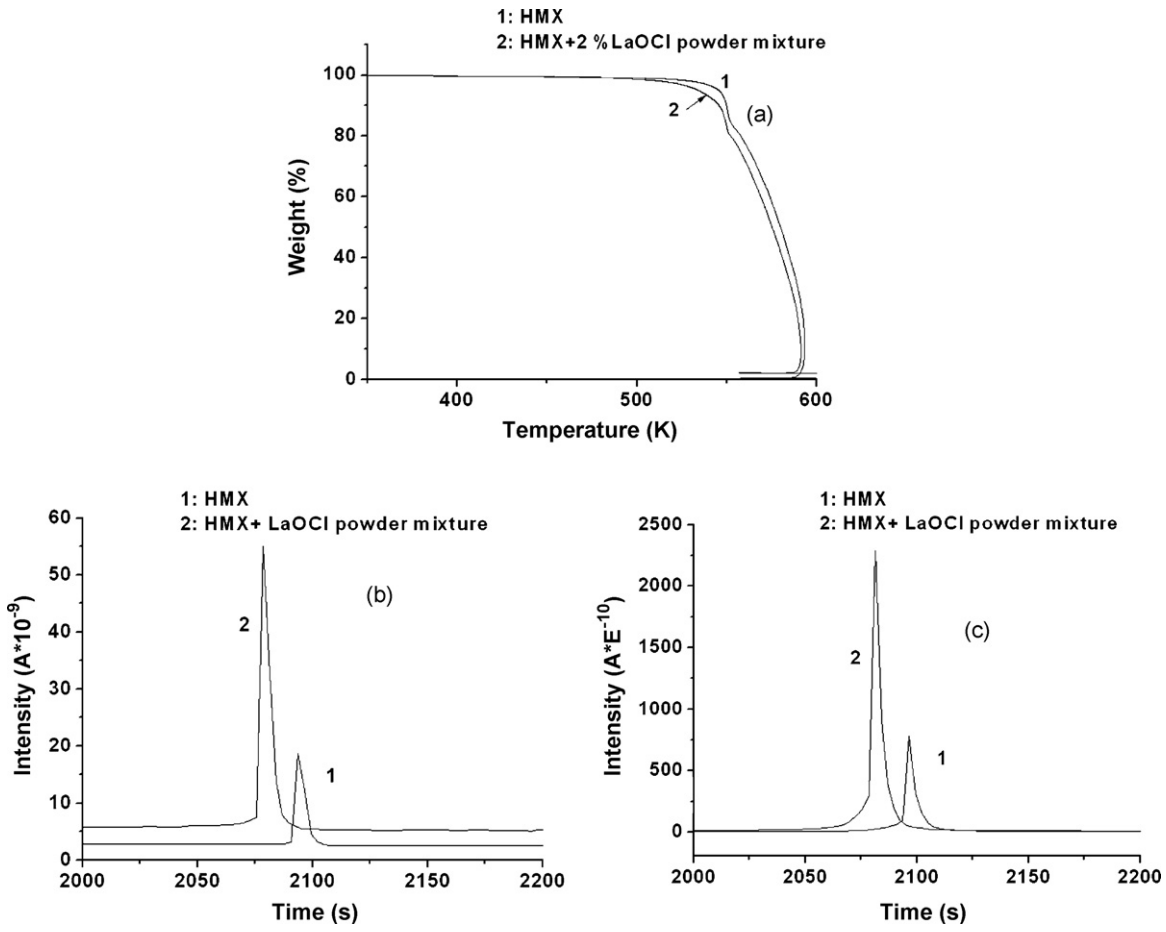

Fig. 7. Results of TG–EGA: TG curves (a), analysis results for release chosen gaseous products HCN (b) and for release chosen gaseous products NO and HCHO (c).

H_2O and O_2, which may come from surface-adsorbed H_2O, OH^- and adsorbed oxygen (O_{ad}), could abstract the hydrogen atoms from HMX, resulting in weakening the bond strength of the adjacent N–N bond, thus causing the NO_2 group to leave easily and catalyzing HMX thermal decomposition. LaOCl powder mixture with high specific surface area has more surface-adsorbed species (see Fig. 5), therefore it could release more surface-adsorbed species and has higher catalytic activity on the early stages of HMX thermal decomposition. It has been proved that surface-adsorbed $La_2O_2CO_3$ has no catalytic performance for HMX thermal decomposition [11]. Therefore, one can infer that surface-adsorbed oxygen (O_{ad}) and hydroxyl could play key roles in the early stages of HMX thermal decomposition, in agreement with the previous result [11].

Further, with increasing temperature, some surface-adsorbed species were desorbed and exposed lattice species such as Mn ion, lattice oxygen and oxygen vacancies. It is reported that Mn ions, the lattice oxygen and oxygen vacancies in perovskite-type oxides are responsible for the oxidation reaction of CO and the reaction between CO and NO [22,23]. They facilitate the adsorption of reactants and catalyze these reactions. Note that CO and NO_x are also two major products of HMX thermal decomposition [24], therefore, $LaMnO_3$ with more lattice oxygen (see Fig. 5) may accelerate the oxidation reaction of CO and the reaction between CO and NO during HMX thermal decomposition, result in the obvious reduction of activation energy and catalyze HMX thermal decomposition.

For perovskite-type oxides ABO_3, oxygen vacancies can be generated by A-site replacements and through the modification of B-site ion oxidation states by ion substitutions in A- and/or B-sites. As a result of the combined effect, one can design and prepare perovskite-type oxides with more active oxygen and hydroxyl species. Thus, though $LaMnO_3$ has lower catalytic activity on the early stages of HMX thermal decomposition in this study, studies based on combinatorial perovskite-type oxide catalysis for HMX thermal decomposition are in progress in our laboratory.

4. Conclusion

Perovskite-type $LaMnO_3$ and LaOCl powder mixture with high specific surface areas were prepared by stearic acid gel combustion route. HMX catalytic thermal decomposition reveals that both perovskite-type $LaMnO_3$ and LaOCl powder mixture have the catalytic activities, and LaOCl powder mixture has much higher catalytic activity than $LaMnO_3$ on the early stages of HMX thermal decomposition. That could be attributed to the higher surface adsorption oxygen (O_{ad}) and hydroxyl as well as its high specific surface area. $LaMnO_3$ obviously reduce activation energy of HMX thermal decomposition. This may be due to its catalytic activity on the oxidation reaction of CO and the reaction between CO and NO during HMX thermal decomposition. The study points out a potential way to develop new and more active catalysts for the HMX thermal decomposition.

Acknowledgements

This project was supported by the Natural Science Fund Council of China (NSFC, nos. 20671084, 20671011 and 20731002).

References

[1] P. Dinka, A.S. Mukasyan, J. Power Sources 167 (2007) 472–481.

[2] A.E. Giannakas, A.K. Ladavos, P.J. Pomonis, Appl. Catal. B: Environ. 49 (3) (2004) 147–158.
[3] A. Delmastro, D. Mazza, S. Vallino Ronchetti, M. Spinicci, R. Brovetto, M.P. Salis, Mater. Sci. Eng. B-Solid State Mater. Adv. Technol. 79 (2001) 140–145.
[4] E. Campagnoli, A. Tavaresb, L. Fabbrini, I. Rossetti, Yu.A. Dubitsky, A. Zaopo, L. Forni, Appl. Catal. B: Environ. 55 (2005) 133–139.
[5] A. Civera, G. Negro, S. Specchia, G. Saracco, V. Specchia, Catal. Today 100 (2005) 275–281.
[6] M.B. Talawar, P.S. Makashir, J.K. Nair, S.M. Pundalik, T. Mukundan, S.N. Asthana, S.N. Singh, J. Hazard. Mater. A 125 (2005) 17–22.
[7] J.F. Li, F.M. Si, Ener. Mater. (Chin.) 10 (2002) 4–9.
[8] J.F. Li, F.M. Si, J. Ener. Mater. (Chin.) 10 (2002) 4–9.
[9] Z.R. Liu, C.M. Yin, Y. Liu, F.Q. Zhao, Y. Luo, Ener. Mater. (Chin.) 13 (2005) 278–283.
[10] R.S. Stepanov, L.A. Kruglyakova, A.M. Astakhov, K.V. Pekhotin, Combust. Explos. Shock Waves 40 (2004) 576–579.
[11] Z.X. Wei, Y.Q. Xu, H.Y. Liu, C.W. Hu, J. Hazard. Mater. 165 (2009) 1056–1061.
[12] B.M. Nagabhushana, R.P. Sreekanth Chakradhar, K.P. Ramesh, C. Shivakumara, G.T. Chandrappa, Mater. Chem. Phys. 102 (2007) 47–52.
[13] A. Civera, M. Pavese, G. Saracco, V. Specchia, Catal. Today 83 (2003) 199–211.
[14] L. Wu, C.Y. Jimmy, L.Z. Zhang, X.C. Wang, S.K. Li, J. Solid State Chem. 177 (2004) 3666–3674.
[15] V.G. Milt, R. Spretz, M.A. Ulla, E.A. Lombardo, J.L. García Fierro, Catal. Lett. 42 (1996) 57–63.
[16] S. Perera, A. Zelenski, R.E. Pho, E.G. Gillan, J. Solid State Chem. 180 (2007) 2916–2925.
[17] X. Gao, D. Dollimore, Thermochim. Acta 215 (1993) 47–63.
[18] Z.R. Liu, C.M. Yin, Y. Liu, X.P. Fan, F.Q. Zhao, Chin. J. Explos. Propell. (Chin.) 27 (2004) 72–79.
[19] Richard Behrens Jr., J. Phys. Chem. 94 (1990) 6706–6718.
[20] Y. Oyumi, T.B. Brill, Combust. Flame. 62 (1985) 213–224.
[21] M.A. Peña, J.L.G. Fierro, Chem. Rev. 101 (2001) 1981–2018.
[22] P.Y. Lin, Y.L. Fu, S.M. Yu, J. Catal. (Chin.) 2 (1981) 186–193.
[23] R.D. Zhang, A. Villanueva, H. Alamdari, S. Kaliaguine, J. Mol. Catal. A: Chem. 258 (2006) 22–34.
[24] P.E. Gongwer, T.B. Brill, Combust. Flam. 115 (1998) 417–423.